

Persistence in Ozone Scaling under the Hurst Exponent as an Indicator of the Relative Rates of Chemistry and Fluid Mechanical Mixing in the Stratosphere

A. F. Tuck,^{*,†} S. J. Hovde,^{†,‡} and M. H. Proffitt^{†,‡,§}

NOAA Aeronomy Laboratory, Boulder, Colorado 80303-3328, CIRES, University of Colorado, Boulder, Colorado 80309, and WMO, Geneva CH-1211, Switzerland

Received: May 18, 1999; In Final Form: August 17, 1999

The observed self-affine fractal behavior of ozone, wind, and temperature in the stratosphere is used to produce an indication of the rate of occurrence of chemistry relative to that of fluid mixing which, unlike the usual method, is independent of an assumed mechanism sequence of elementary chemical steps followed by application of the law of mass action to obtain differential equations describing the temporal and spatial evolution of the reacting gases. Rather, the occurrence of chemistry is deduced from the scaling of the observed variability; it is applied empirically to deduce the presence of chemical processes that are faster than fluid mechanical mixing above an altitude of 19 km during a balloon flight, and in the Antarctic spring, Arctic summer, and Arctic winter during high altitude aircraft flights. The method should apply to any volume of reacting molecules to which the equations of fluid motion apply and for which measurements can be made over a range of scales.

Introduction

It has been the practice to identify the occurrence of chemistry in the atmosphere by proposing a mechanism, often deduced from the presence of observed source species, applying the law of mass action, and integrating the resulting set of differential equations forward, thus expressing the molecular concentrations at a point as a function of time. These predicted concentrations may then be tested by observation. While this is frequently successful, particularly, for example, in the case of the upper stratosphere, there is in many cases substantial doubt. This doubt arises from the fact that the chemistry often proceeds at about the same rate or slower than fluid mechanical processes of transport and mixing.¹ There thus is value in obtaining an indication of the occurrence of chemistry by direct inference from observations, independent of application of the law of mass action to a posited reaction mechanism of elementary collisional steps.

Recently, it has been shown² that ozone, wind, and temperature measured from the ER-2 high-altitude aircraft behave as self-affine fractals in the lower stratosphere. These quantities were shown to obey single exponent scaling over 4 orders of magnitude in horizontal length scale, up to one Earth radius (~6900 km) under the Hurst exponent,^{3,4} H_1 , as computed by the first-order technique of rescaled range analysis.⁵ Here we show that ozone displays persistence, $H_1 \geq 0.60$, in circumstances where its Hurst exponent is greater than that of the horizontal wind speed; in the great majority of ER-2 observations to date, both wind speed and ozone had H_1 close to the random value⁶ of 0.50. We note that in principle the Hurst exponent technique may be applied to any volume in which fluid mechanical assumptions are valid, a scale as small as 10^{-5} m^{7,8} at STP in air; it is only necessary to have good enough observations over a wide enough range of scales. In fact, since Brownian motion is fractal with $H_1 = 0.5$, it would work down

to the scale of a mean free path—if an experimental technique was available. In this work, the range of scales is obtained in the vertical by 1 Hz observations from a balloon ascending at 5 m s⁻¹ between 0 and 40 km and in the horizontal by 1 Hz observations from an aircraft flying at 200 m s⁻¹ for up to 10.3 h. The technique works best over great circle tracks flown horizontally without vertical excursions, although scaling still occurs during aircraft climbs and dives.

The application of fractal analysis to atmospheric data was pioneered by Lovejoy⁹ for cloud area–perimeter relationships and has been extended into multifractal techniques by Schertzer, Lovejoy, and their collaborators.^{10–12} They have developed a universal multifractal scheme that uses a three-parameter description and have employed it to question the existence of an atmospheric transition from two-dimensional to three-dimensional turbulence at mesoscales (order 10² km). Bifractal analysis and the use of high-order structure functions was used to investigate radiative transfer in stratocumulus clouds by Davis and collaborators.¹³ Schertzer and Lovejoy have made a start on generating structures of the kind observed in the atmosphere via multifractal cascade dynamics and turbulent intermittency.¹² These references should be consulted for a guide to the application of fractal techniques to atmospheric observations.

Methods

We employ many time series of ozone observed from the NASA ER-2 high-altitude aircraft^{14,15} during three missions that investigated ozone photochemistry in polar regions and one observed by essentially the same instrument¹⁶ during a high-altitude balloon ascent to 3 hPa (40 km altitude). The ER-2 missions were the Airborne Antarctic Ozone Experiment (AAOE),¹⁷ the Airborne Arctic Stratospheric Experiment (AASE),¹⁸ and the Photochemistry of Ozone Loss in Arctic Regions in Summer (POLARIS),¹⁹ which took place respectively during August–September 1987 from Punta Arenas (53° S, 71° W), January–February 1989 from Stavanger (59° N, 6° E), and April–September 1997 from Fairbanks, AK (65° N, 148° W). The rescaled range analysis for H_1 has been described previ-

* Corresponding author. E-mail: tuck@al.noaa.gov.

† NOAA Aeronomy Laboratory.

‡ CIRES.

§ WMO.

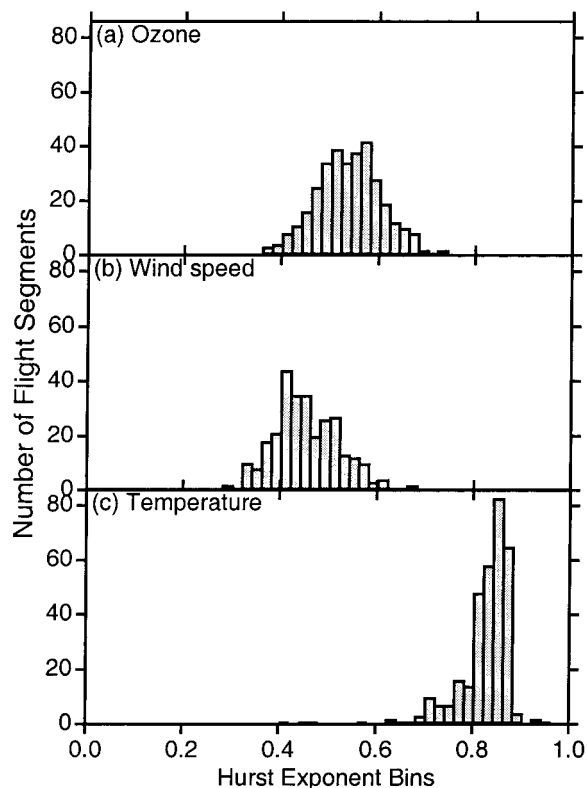


Figure 1. Histograms of the Hurst exponent from all qualifying ER-2 horizontal segments (334 from 191 flights) between January 1987 and September 1997 for (a) ozone, (b) wind speed, and (c) temperature.

ously, as have histograms giving H_1 for ozone, wind speed, wind direction, vertical wind speed, and temperature.² The most frequent value of $H_1(\text{O}_3)$ was 0.57 with a median of 0.54; those for wind speed, $H_1([u^2 + v^2]^{0.5})$, where u = eastward velocity and v = northward velocity, were 0.41 and 0.46, respectively, while for temperature $H_1(T)$ the values were 0.85 and 0.84. Those results came from four missions and used 170 horizontal flight segments from 95 flights. Values here were derived from eight ER-2 missions spanning all seasons, latitudes from 72° S to 90° N, and longitudes from 15° E through 180° W to 165° E between January 1987 and September 1997. A total of 334 horizontal flight segments from 191 flights were used; all were in the stratosphere and of at least 1500 s duration. The histograms for $H_1(\text{O}_3)$, $H_1([u^2 + v^2]^{0.5})$, and $H_1(T)$ are shown in Figure 1. Where ozone was a self-affine random fractal ($H_1 \approx 0.50$) we relate this, on an empirical and intuitive basis, to the near random fractal behavior of the wind speed; physically, the speed shear of the horizontal wind leads to the exponential stretching and distortion of ozone mixing ratio isosurfaces when the chemistry is too slow to compete. We note that relating the production of sharp gradients and filaments to the Navier–Stokes equation for fluid motion on the rotating Earth is a difficult endeavor.¹² When the added complexity of the equations describing chemical evolution is considered, it will probably be some time before the physical interpretation of empirical scaling exponents is on a mathematically secure footing. H_1 values for ozone and wind speed ≈ 0.5 are the case in much of the lower stratosphere, as witnessed by the similarity of the histograms in Figure 1a,b. Note, however, that the ozone histogram is positioned about 0.1 toward the high end of the Hurst exponent axis, which ranges from zero to unity, relative to the histogram for wind speed. The low wing of the ozone histogram, values less than about 0.45, corresponds to sharp gradients at filament edges;² new filamentation causes antiper-

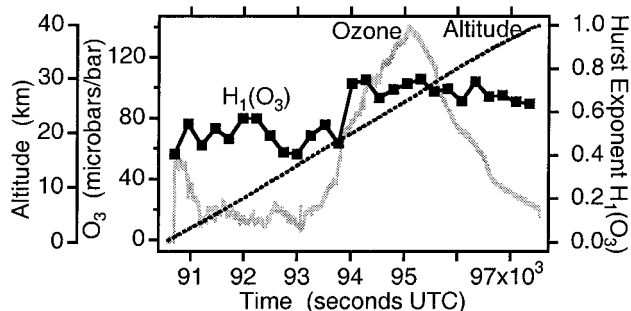


Figure 2. Large balloon flight, ascent from the surface to 40 km at (32° N, 96° W) on 19831010. The abscissa is time in UTC seconds. The ordinates are ozone partial pressure (solid curve), balloon altitude (dotted), and Hurst exponent $H_1(\text{O}_3)$ over 256 s intervals (dots joined by lines). Note the transition at 19 km in $H_1(\text{O}_3)$ from random values (≈ 0.50) to persistent values (≈ 0.65).

sistence in $H_1(\text{O}_3)$, lowering the values below the random number of 0.5. It should be noted also that there is a number of flight segments with values of $H_1(\text{O}_3) \geq 0.60$ with no counterpart in the $H_1([u^2 + v^2]^{0.5})$ histogram. It is upon these flights that we will concentrate: many of those involving long flight segments occurred in the Arctic during summer 1997, with the remainder occurring in late August–early September 1987 in the Antarctic vortex and during January–February 1989 in the Arctic vortex. We also use the balloon flight to 40 km to demonstrate the existence of a sharp transition in the vertical between a tropospheric–lower stratospheric regime where $H_1(\text{O}_3)$ is random and the region above it to 40 km, in which $H_1(\text{O}_3)$ is persistent.

Results

Figure 2 displays the time series of ozone measured during the large balloon flight of 19831010 (yyyymmdd date format) from Palestine, TX (32° N, 96° W), along with the altitude of the balloon. Also plotted is the trace of $H_1(\text{O}_3)$, evaluated² at intervals of 256 s. This interval was chosen as the smallest over which the scaling was arithmetically adequate, in an attempt to examine structure above and below the primary change in regime located at 19–20 km. Below 19 km, $H_1(\text{O}_3)$ varies somewhat about a mean close to the random value of 0.50, while above 19 km, the value of $H_1(\text{O}_3)$ transitions to a value of about 0.65: at 19 km, there is a sharp change in ozone behavior. Above this altitude, ozone behaves as a persistent self-affine fractal, while below it, it is a random self-affine fractal. It has long been calculated in numerical models of stratospheric composition that there is a change from a photochemically dominated regime in the upper stratosphere to a dynamically dominated regime beneath, but the altitude at which this occurs has been usually given as considerably higher than 19 km. The altitude as deduced from, for example, correlation between the mean profiles of ozone and potential vorticity has been given²⁰ as ~ 24 km, and as ranging from 20 km in the tropics to 40 km at the poles based on calculation.²¹ We note that the in situ data used here are of very low noise, have high time resolution, and are accurately calibrated;^{14,16} the balloon instrument provides 5 m vertical resolution since the ascent is at 5 m s⁻¹ and the instrument has 1 Hz time response. These characteristics should allow a more accurate study of the variability and scaling. Although we are not concerned here with the second-order structure of $H_1(\text{O}_3)$ in Figure 2, we note that detailed investigation of the vertical scaling using multifractal techniques may prove fruitful in the future, if additional scaling regimes in fact exist.

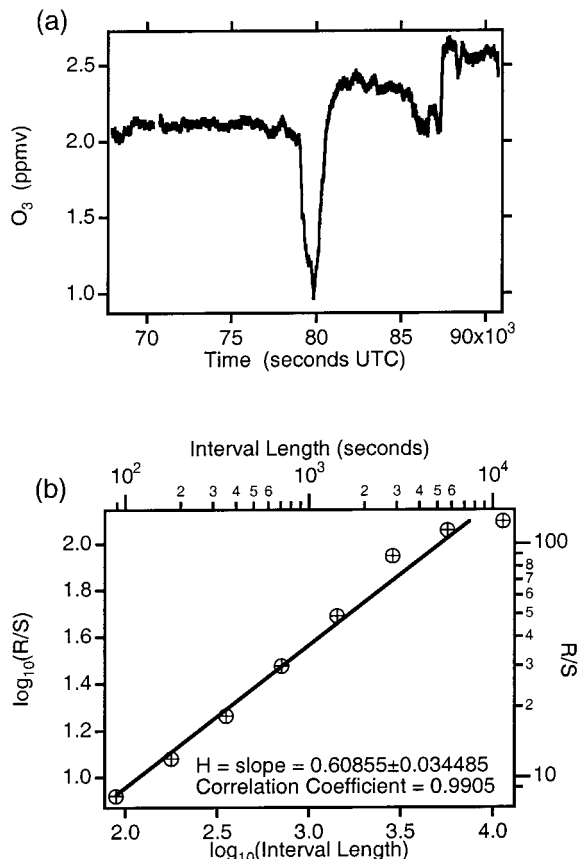


Figure 3. (a) Trace of ozone mixing ratio vs time, taken by the ER-2 in the Arctic lower stratosphere on 19970707 between (65° N, 148° W) and 90° N and return. (b) log-log plot from rescaled range analysis² of the data in (a), the slope of which is the Hurst exponent $H_1(\text{O}_3)$.

Having empirically associated persistence in $H_1(\text{O}_3)$ with a regime in which photochemistry outpaces mixing, we now examine the aircraft data. The ER-2 flies at a velocity close to 200 m s^{-1} , so the 1 Hz data from the aircraft represent a factor of 40 more in length scale horizontally than the balloon's 5 m s^{-1} in the vertical. Figure 3a represents an ER-2 ozone time series obtained 19970707 during a flight from Fairbanks to the North Pole and back. The log-log plot for the northbound flight segment, from which $H_1(\text{O}_3)$ was obtained, is shown in Figure 3b. The rescaled range analysis² has taken the data from Figure 3a and transformed it to the straight line in Figure 3b. Note that $H_1(\text{O}_3) = 0.61$, a persistent value on the high wing of the histogram in Figure 1a. More spectacular examples² have shown that even the wildly variable ozone mixing ratios seen at middle and high latitudes in winter and spring can be transformed into straight lines. This indicates that the variability can be described by a single power law exponent; this exponent can then be associated empirically with different regimes of chemistry and mixing. The values of $H_1(\text{O}_3)$ seen in the Arctic between April and September 1997 are shown in Figure 4. It is clear that in spring and autumn the values of $H_1(\text{O}_3)$ fall in the middle of the histogram (Figure 1a) but that in midsummer the values are persistent. Reinforced by the balloon profile, we suggest that this indicates the occurrence of chemistry in midsummer which is proceeding faster than the wind speed can impose randomness, or even some antipersistence, in the fractal scaling, and so succeeds in producing persistence in the ozone. Persistence means that there is positive correlation among neighboring data intervals, on all scales.² The mean value of $H_1([u^2 + v^2]^{0.5})$ for the same flights remained essentially unchanged at about 0.42 throughout the Arctic spring, summer,

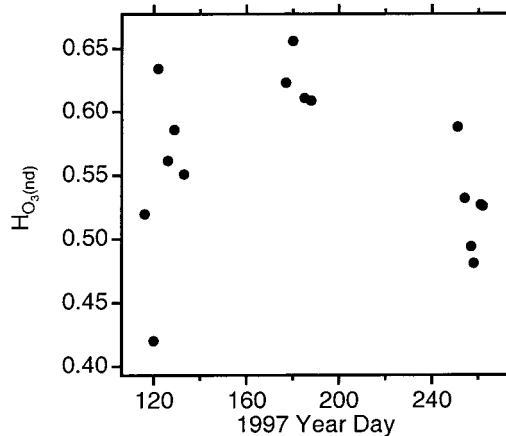


Figure 4. Values of the Hurst exponent, $H_1(\text{O}_3)$, from all usable ER-2 stratospheric flight segments between the end of climb after take off and the beginning of descent before landing, taken in the Arctic between April and September 1997. Number densities were used in the calculation. There is randomness in spring and autumn, persistence in midsummer.

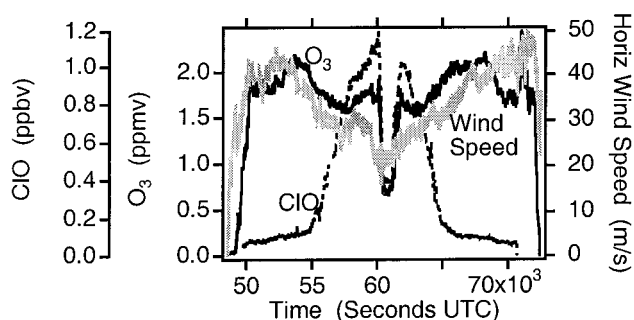


Figure 5. Data from an ER-2 flight into the Antarctic vortex on 19870830. The ozone trace is the solid line, the ClO is dotted, and the wind speed is gray. Hurst exponents for ozone number density were evaluated for the two horizontal segments inside the vortex, poleward of the points where ClO = 100 pptv and separated by the dive and climb maneuver in the middle of the flight.

and autumn. The midsummer persistence is therefore concluded to originate with photochemistry, since the wind demonstrates continued randomness or even a small degree of antipersistence from spring to fall.

Another location where $H_1(\text{O}_3) \geq 0.60$ was observed was in the Antarctic vortex in late August and early September 1987. Typical traces of ozone¹⁴ and chlorine monoxide²² are shown in Figure 5, along with the wind speed.²³ Poleward of the wind speed maximum, ClO increases dramatically by more than 1 order of magnitude and ozone drops by up to 30%, characteristic signatures of the ozone hole. For 9 of the 10 flights from 19870823 to 19870922 the horizontal segments of the flight track (two in number, on either side of a dive and climb in the middle of the flight) which were inside the vortex ($\text{ClO} \geq 100 \text{ pptv}$) were analyzed for $H_1(\text{O}_3)$. The flight of 19870921 had too short a track in the vortex region of gross chemical perturbation to provide a reliable calculation of Hurst exponents. The resulting time behavior of the Hurst scaling exponent from late August to late September is shown in Figure 6. In late August, there is persistence; $H_1(\text{O}_3)$ is greater than 0.60. By late September, $H_1(\text{O}_3)$ has declined, approaching the random value of 0.50. The decline is significant; recall that such a transition characterized the balloon data above and below 19 km, and also the difference in the Arctic aircraft data between midsummer on one hand and spring and autumn on the other. The value of $H_1([u^2 + v^2]^{0.5})$ remained near the mean value of

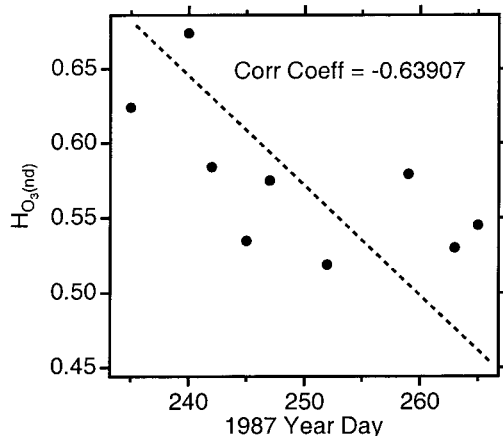


Figure 6. Hurst exponents $H_1(\text{O}_3)$ for vortex ozone, evaluated as in Figure 5, plotted for 9 of the 10 flights from 19870823 to 19870922. The flight of 19870921 had an insufficiently long track in the high CIO region to yield an accurate Hurst exponent. Note the decline from persistence in late August toward randomness in late September; although the linear fit extends to values of $H_1(\text{O}_3)$ less than 0.50 in late September, such values were not observed.

0.49 throughout the sequence of 10 flights, showing that the scaling of the wind speed was unchanged while that of the ozone changed from persistent toward random.

We consider also the Arctic winter vortex,^{18,24} in which the ER-2 completed 14 flights in January and February 1989. Figure 7 shows a plot of $H_1(\text{O}_3)$ vs $H_1([u^2 + v^2]^{0.5})$, evaluated² for flight segments both inside and outside the vortex. It may be seen that the points representing flight segments inside the vortex lie above the 1:1 line, i.e., that $H_1(\text{O}_3) > H_1([u^2 + v^2]^{0.5})$. The points representing flight segments exterior to the vortex tend to lie along the 1:1 line, with a few points above it. The latter probably represent air equatorward of the wind maximum which has experienced PSC processing.¹⁸ The small number of points significantly below the 1:1 line can be traced to the flight of 19890120; it is not known if the cause is instrumental problems or an unusual atmospheric condition. The time series of $H_1(\text{O}_3)$ for air inside the vortex fluctuates during the period of the mission, with large values following PSC episodes by a few days between 19890103 and 19890210. This behavior suggests that continual PSC processing may be necessary to maintain a fully processed vortex over a period of a week or more.

Discussion and Conclusions

We suggest that the occurrence of persistence in stratospheric ozone, as indicated by the Hurst scaling exponent $H_1(\text{O}_3) \geq 0.60$, is induced in certain locations by photochemical reactions that proceed more rapidly than the randomizing effects of wind speed and its shear can maintain $H_1(\text{O}_3) \approx H_1([u^2 + v^2]^{0.5}) \approx 0.5$. Intuitively, this is reasonable: in such locations as the summertime Arctic or the subtropical upper stratosphere at autumn turnaround the stratosphere is characterized by low wind speeds (generally $< 10 \text{ m s}^{-1}$) and slack gradients. The photochemistry consists of a sequence of elementary steps, which in the atmosphere tend to have low activation energies. Chemical reaction will thus tend to produce positive correlation in neighboring volumes of the stratosphere, resulting in the observed persistence, by tending to move toward a common photoequilibrated state characteristic of the region containing the volumes. The mechanism will propagate at all scales, from that of the molecular mean free path upwards, and might thus be expected to maintain fractal scaling while producing persistence, as observed. We may also regard the persistent value of

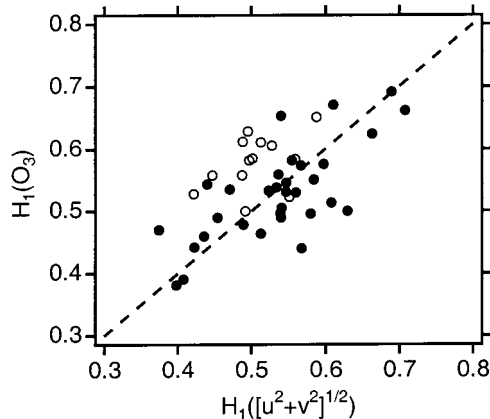


Figure 7. $H_1(\text{O}_3)$ vs $H_1([u^2 + v^2]^{0.5})$. The open circles refer to the flight segments poleward of the wind speed maximum (inside the vortex), while the filled circles refer to those equatorward of the wind speed maximum (outside the vortex).

0.65 for $H_1(\text{O}_3)$ as intermediate between the $H_1([u^2 + v^2]^{0.5})$ of ≈ 0.42 and the $H_1(\text{T})$ of ≈ 0.85 . These two represent the basic physical effects whose interplay determines the ozone scaling. On one hand, temperature is the macroscopic manifestation of molecular motion—the translational energy of the molecules that is expressed via the Maxwell–Boltzmann distribution and that equilibrates at every collision; it is therefore nonconservative. For a molecule affected by a chemical process that occurred at every collision, we might expect a Hurst exponent equal to that of temperature. On the other hand, in practice, the randomizing effect of wind speed and its shear reduce it to the lower values actually observed. The occurrence of activation energies in the chemical steps will also slow the chemistry and reduce $H_1(\text{O}_3)$ compared to $H_1(\text{T})$. However, we note that the present empirical analysis is the simplest possible and that more sophisticated schemes using multifractal techniques^{11,12} or higher order structure functions¹³ may well reveal more subtle interpretations. As we have noted, secure mathematical linkages between the governing equations for reacting air on the rotating Earth and the generation of the observed scale invariant structures in chemicals and meteorological variables have not been demonstrated.

The observation of persistence in the Antarctic vortex ozone in late August and early September, followed by a decline during September toward randomness may offer interesting insights into the behavior of the chlorine-mediated loss occurring there.^{22,25} We suggest the following interpretation. The transformation of chlorine from the ozone-inactive forms (HCl, ClONO₂) to the active ones (Cl₂, Cl, ClO, Cl₂O₂, HOCl) starts to occur well before midwinter, probably about 6 weeks before solstice^{26,27} with ozone loss of $\sim 25\%$ occurring in the sunlit outer vortex between early June and early August.^{28,29} The spatial and temporal incidence of the polar stratospheric clouds, which are the agents of such chlorine activation, peaks in August, declining through September, and ceasing in October.^{30–32} Thus, in late August it is reasonable to expect ozone to be persistent, reflecting the ability of the frequent PSC processing to maintain a fully processed vortex with the concomitant high and relatively uniform abundance of CIO and ozone, the latter of which is in decline but not yet lost. However, as the PSC frequency declines through September, some extra variability may occur, arising from variably longer periods since air parcels were in a PSC and from the resupply of unprocessed air in the mixing zone centered on the jet stream core.^{33–35} The high wind shears on all scales in this region (Figure 5) are what cause the

near random value of $H_1[(u^2 + v^2)^{0.5}] \approx 0.49$, which was observed from late August to late September. Note that this interpretation does not imply a cessation of ozone loss chemistry or low average ClO by late September; what it does imply is a decline in the rate of the ozone loss chemistry relative to the rate of the fluid mechanical mixing. While the occurrence of photochemical ozone loss has been demonstrated beyond doubt in the Antarctic vortex,^{22,25,36} it is less obvious for the other regimes considered here: the 1989 winter vortex and the 1997 summer anticyclone in the Arctic. We offer the observed persistence of ozone scaling in these locales, in the presence of steady randomness in the scaling of wind speed, as an argument that the ozone photochemistry is outpacing the mixing and transport. This result is in accord with earlier analyses^{24,36} using nitrous oxide–ozone correlation in the Antarctic spring and in the Arctic winter.

It is perhaps surprising that the wind speed shows only a small tendency to exhibit persistence, even during flights along and across the polar night jet stream. The smooth wind profile often assumed in large scale dynamical meteorology would in the limit give an H_1 of unity; this is never seen in the ER-2 data, and the reality was foreshadowed by Richardson,³⁷ who asked, “Does the wind possess a velocity?”, and commented, “This question, at first sight foolish, grows on acquaintance”. Inspection of the 1 Hz structure in the observed jet stream wind profiles, in both speed and direction, reveals the kinematic inevitability of the generation of gradients and structure on all scales. There is no reason to expect much persistence in the wind, an expectation fulfilled in Figures 1b and 7.

We note that this technique can be applied to any volume large enough for the assumptions of fluid mechanics to be obeyed, a scale of about 10^{-5} m at STP according, for example, to Batchelor⁷ and Hirschfelder, Curtiss, and Bird.⁸ In the case of the stratosphere, the relative dimensions of the Earth and the ER-2's range allow coverage over 4 orders of magnitude for a 1 Hz instrument with a continuous data record and with adequately small random error. These conditions are met by the measurements of ozone, and often by those of wind and temperature, but not currently by other instruments.² The ozone has abundances and characteristic chemical time scales that make it the optimal molecule for the length scales accessible by the aircraft. The method is at its best when applied to long, isentropic, great circle flight tracks uninterrupted by vertical excursions; in such cases, the time axis is directly transformable to a length scale, the dynamical information is clearest, and the Hurst exponent scaling works better the longer the data record. It would be extremely interesting if faster time response and a continuous data record could be achieved by the instruments^{19,22,38} measuring the chain-carrying species such as ClO, NO, NO₂, OH, and HO₂; the correlations and their scaling as diagnosed by H_1 should provide direct light on the occurrence of the elementary steps. Given the instrumentation, in fact, persistence vs randomness as a signature of chemical change should work on scales all the way down to the mean free path, since Brownian motion is a random self-affine fractal.^{4,6} In a complex reacting mixture, a Hurst exponent of 0.5 for a particular species would indicate either no participation or participation on a catalytic basis. Persistence or antipersistence would indicate a change in the mole fraction in space and time, attributable to chemical production or loss. Interpolation between the collision rate giving a Hurst exponent equal to that for temperature and the Hurst exponent equal to that for wind speed corresponding to zero should in principle permit the direct extraction of chemical rate information.

Finally, we remark that our technique needs precise, accurate, and fast data and that it is applicable along individual aircraft and balloon trajectories of sufficient length. In this respect, it is different from the classical Gaussian second moment technique of using the relative dispersion³⁹ (standard deviation divided by the mean) that combines data from disparate sources, often on a global scale; given fractal behavior, there is no guarantee that Gaussian statistics will work, because a few outliers may then determine the mean or higher moments of the integrals may not converge.^{10,40} More sophisticated multifractal analysis^{10–13} may yield more refined or subtle interpretations; in the meantime, single scaling exponent analysis offers a consistent empirical interpretation of the observations. Persistence in ozone is observed where photochemistry has been calculated to be important—in the winter/spring vortices, in the polar summer anticyclone, and in the upper stratosphere. It is therefore a useful method for diagnosing empirically the occurrence of chemistry without recourse to a numerical model.

References and Notes

- (1) Tuck, A. F.; Proffitt, M. H. *J. Geophys. Res.* **1997**, *103*, 28215.
- (2) Tuck, A. F.; Hovde, S. J. *Geophys. Res. Lett.* **1999**, *26*, 1271.
- (3) Hurst, H. E. *Trans. Am. Soc. Civ. Eng.* **1951**, *116*, 770.
- (4) Mandelbrot, B. B. *The Fractal Geometry of Nature*; W. H. Freeman: New York, 1982; Chapter IX.
- (5) Bassingthwaite, J. B.; Raymond, G. M. *Ann. Biomed. Eng.* **1994**, *22*, 432.
- (6) Hastings, H. M.; Sugihara, G. *Fractals: A User's Guide*; Clarendon Press: Oxford, U.K., 1993; Chapter 2.
- (7) Batchelor, G. K. *An Introduction to Fluid Mechanics*; Cambridge University Press: Cambridge, U.K., 1967; Chapter 1.
- (8) Hirschfelder, J. O.; Curtiss, C. F.; Bird, R. B. *The Molecular Theory of Gases and Liquids*, 2nd ed.; John Wiley: New York, 1964; Chapters 7 and 11.
- (9) Lovejoy, S. *Science* **1982**, *216*, 185.
- (10) Schertzer, D.; Lovejoy, S. *Turbulent Shear Flows 4*; Springer, New York, 1985; pp 7–33.
- (11) Lazarev, A.; Schertzer, D.; Lovejoy, S.; Chigirinskaya, Y. *Nonlinear Processes Geophys.* **1994**, *1*, 115.
- (12) Schertzer, D.; Lovejoy, S.; Schmitt, F.; Chigirinskaya, Y.; Marsan, D. *Fractals* **1997**, *5*, 427.
- (13) Davis, A. B.; Marshak, A.; Cahalan, R. F.; Wiscombe, W. J. *Fractals* **1997**, *5*, 129.
- (14) Proffitt, M. H.; Steinkamp, M. J.; Powell, J. A.; McLaughlin, R. J.; Mills, O. A.; Schmeltekopf, A. L.; Thompson, T. L.; Tuck, A. F.; Tyler, T.; Winkler, R. H.; Chan, K. R. *J. Geophys. Res.* **1989**, *94*, 16547.
- (15) Tuck, A. F.; Baumgardner, D.; Chan, K. R.; Dye, J. E.; Elkins, J. W.; Hovde, S. J.; Kelly, K. K.; Loewenstein, M.; Margitan, J. J.; May, R. D.; Podolske, J. R.; Proffitt, M. H.; Rosenlof, K. H.; Smith, W. L.; Webster, C. R.; Wilson, J. C. *Q. J. R. Meteorol. Soc.* **1997**, *123*, 1.
- (16) Proffitt, M. H.; McLaughlin, R. J. *Rev. Sci. Instrum.* **1983**, *54*, 1719.
- (17) Tuck, A. F.; Watson, R. T.; Condon, E. P.; Margitan, J. J.; Toon, O. B. *J. Geophys. Res.* **1989**, *94*, 11181.
- (18) Tuck, A. F.; Davies, T.; Hovde, S. J.; Noguer-Alba, M.; Fahey, D. W.; Kawa, S. R.; Kelly, K. K.; Murphy, D. M.; Proffitt, M. H.; Margitan, J. J.; Loewenstein, M.; Podolske, J. R.; Strahan, S. E.; Chan, K. R. *J. Geophys. Res.* **1992**, *97*, 7883.
- (19) Gao, R. S.; Fahey, D. W.; Del Negro, L. A.; Donnelly, S. G.; Keim, E. R.; Neuman, J. A.; Teverovskaia, E.; Wennberg, P. O.; Hanisco, T. F.; Lanzendorf, E. J.; Proffitt, M. H.; Margitan, J. J.; Wilson, J. C.; Elkins, J. W.; Stimpfle, R. M.; Cohen, R. C.; McElroy, C. T.; Bui, T. P.; Salawitch, R. J.; Brown, S. S.; Ravishankara, A. R.; Portmann, R. W.; Ko, M. K. W.; Weisenstein, D. K.; Newman, P. A. *Geophys. Res. Lett.* **1999**, *26*, 1153.
- (20) Danielsen, E. F. *Ozone in the Free Atmosphere*; Van Nostrand Reinhold: New York, 1985; Chapter 4.
- (21) Wayne, R. P. *Chemistry of Atmospheres*, 2nd ed.; Clarendon Press: Oxford, U.K., 1991; Chapter 4.
- (22) Anderson, J. G.; Brune, W. H.; Proffitt, M. H. *J. Geophys. Res.* **1989**, *94*, 11465.
- (23) Chan, K. R.; Scott, S. G.; Bui, T. P.; Bowen, S. W.; Day, J. J. *Geophys. Res.* **1989**, *94*, 11573.
- (24) Proffitt, M. H.; Margitan, J. J.; Kelly, K. K.; Loewenstein, M.; Podolske, K. R.; Chan, K. R. *Nature* **1990**, *347*, 31.
- (25) Jones, R. L.; Austin, J.; McKenna, D. S.; Anderson, J. G.; Fahey, D. W.; Farmer, C. B.; Heidt, L. E.; Kelly, K. K.; Murphy, D. M.; Proffitt, M. H.; Tuck, A. F.; Vedder, J. F. *J. Geophys. Res.* **1989**, *94*, 11529.

- (26) Tuck, A. F. *J. Geophys. Res.* **1989**, *94*, 11687.
- (27) Tuck, A. F.; Webster, C. R.; May, R. D.; Scott, D. C.; Hovde, S. J.; Elkins, J. W.; Chan, K. R. *Discuss. Faraday Soc.* **1995**, *100*, 389.
- (28) Tuck, A. F.; Kelly, K. K.; Webster, C. R.; Loewenstein, M.; Stimpfle, R.; Proffitt, M. H. *J. Chem. Soc., Faraday Trans.* **1995**, *91*, 3063.
- (29) Roscoe, H. K.; Jones, A. E.; Lee, A. M. *Science*, **1997**, *278*, 93.
- (30) McCormick, M. P.; Trepte, C. R.; Pitts, M. C. *J. Geophys. Res.* **1989**, *94*, 11241.
- (31) Watterson, I. G.; Tuck, A. F. *J. Geophys. Res.* **1989**, *94*, 16511.
- (32) Fromm, M.; Lumpe, J. D.; Bevilacqua, R. M.; Shettle, E. P.; Hornstein, J.; Massie, S. T.; Fricke, K. H. *J. Geophys. Res.* **1997**, *102*, 23659.
- (33) Murphy, D. M.; Tuck, A. F.; Kelly, K. K.; Chan, K. R.; Loewenstein, M.; Podolske, J. R.; Proffitt, M. H.; Strahan, S. E. *J. Geophys. Res.* **1989**, *94*, 11669.
- (34) Pierce, R. B.; Fairlie, T. D. A.; Grose, W. L.; Swinbank, R.; O'Neill, A. *J. Atmos. Sci.* **1994**, *51*, 2957.
- (35) Bithell, M.; Gray, L. J.; Harries, J. E.; Russell, J. M., III; Tuck, A. F. *J. Atmos. Sci.* **1994**, *51*, 2942.
- (36) Proffitt, M. H.; Kelly, K. K.; Powell, J. A.; Gary, B. L.; Loewenstein, M.; Podolske, J. R.; Strahan, S. E.; Chan, K. R. *J. Geophys. Res.* **1989**, *94*, 16797.
- (37) Richardson, L. F. *Proc. R. Soc.* **1926**, *A110*, 709.
- (38) Wennberg, P. O.; Cohen, R. C.; Hazen, N. L.; Lapson, L. B.; Allen, N. T.; Hanisco, T. F.; Oliver, J. F.; Lanham, N. W.; Demusz, J. N.; Anderson, J. G. *Rev. Sci. Instrum.* **1994**, *65*, 1858.
- (39) Ehhalt, D. H.; Rohrer, F.; Wahner, A.; Prather, M. J.; Blake, D. R. *J. Geophys. Res.* **1998**, *103*, 18981.
- (40) Mandelbrot, B. B. *Fractals and 1/f Noise*; Springer-Verlag: New York, 1998; Chapter N15.